

A 65nm 36nJ/Decision Bio-inspired Temporal-Sparsity-Aware Digital Keyword Spotting IC with 0.6V Near-Threshold SRAM

Qinyu Chen^{1,2,*} Kwantae Kim^{3,4,*} Chang Gao^{5,*} Sheng Zhou¹ Taekwang Jang³ Tobi Delbruck¹ Shih-Chii Liu¹

¹Institute of Neuroinformatics, University of Zürich and ETH Zürich, Switzerland

²Leiden University, The Netherlands

³ETH Zürich, Switzerland

⁴Aalto University, Finland

⁵Delft University of Technology, The Netherlands

*Equal Contribution.

Emails: q.chen@liacs.leidenuniv.nl, shih@ini.uzh.ch

ABSTRACT

This paper introduces, to the best of the authors' knowledge, the first fine-grained temporal sparsity-aware keyword spotting (KWS) IC. This IC leverages temporal similarities between neighboring feature vectors extracted from input frames and network hidden states, eliminating unnecessary operations and memory accesses. The KWS IC features a bio-inspired delta-gated recurrent neural network (Δ RNN) classifier and achieves an 11-class Google Speech Command Dataset (GSCD) KWS accuracy of 90.5% and energy consumption of 36 nJ/decision. At 87% temporal sparsity, computing latency and energy per inference are reduced by 2.4 \times and 3.4 \times , respectively. The 65 nm design occupies 0.78 mm² and includes two additional blocks: a compact 0.084 mm² digital infinite-impulse-response (IIR)-based band-pass filter (BPF) audio feature extractor (FEx) and a 24 kB 0.6 V near- V_{th} weight SRAM with 6.6 \times lower read power compared to standard SRAM.

INTRODUCTION

Keyword spotting (KWS) is crucial for voice-activated devices. KWS integrated circuits (ICs) focus on reducing power in the feature extractor (FEx) and the neural network classifier through weight and activation sparsity. Methods to reduce FEx power include serial fast Fourier transform (FFT) designs, which impact latency¹, and time-domain filtering for process scalability^{2,3}. Besides bit-level weight sparsity, recent ICs report methods using dynamic sparsity, such as in-memory recurrent activation, achieving 70% activation sparsity⁴ and 70% temporal sparsity by skipping input frames⁵.

This paper introduces a sparsity-aware KWS IC featuring three key innovations:

1. A bio-inspired Δ RNN accelerator achieving 2.4 \times latency reduction and 3.4 \times energy per decision reduction.
2. A serial infinite impulse response (IIR) band-pass filter (BPF) FEx achieving 5.7 \times power reduction and 4.7 \times area reduction.
3. A near-threshold-operating full-custom static random-access memory (SRAM) achieving 6.6 \times lower power consumption.

BIO-INSPIRED TEMPORAL-SPARSITY-AWARE KWS SYSTEM

Figure 1 shows the chip architecture with a Δ RNN accelerator, a 24kB near-threshold SRAM for weight storage, and a compact serial IIR BPF-based time-domain FEx. An asynchronous FIFO connects FEx outputs to the Δ RNN accelerator across various clock domains.

Figure 2 presents the Δ RNN's design, inspired by the spiking threshold and low spike rate observed in biological neural networks⁶⁻¹⁰. The Δ RNN leverages fine-grained temporal sparsity by updating only above-threshold neurons across successive frames. It skips redundant computations and memory accesses, remarkably enhancing energy efficiency. It includes a Δ Input layer, a Δ Gated Recurrent Unit (Δ GRU)-based hidden layer, and a final fully-connected (FC) layer for scoring 11 GSCD classes. The Δ RNN comprises a Δ Encoder for temporal difference computation, focusing on significant neuron updates exceeding a defined threshold and achieving a balance between accuracy and energy. It processes non-zero delta states in delta FIFOs (D-FIFOs), using 8 MAC units for efficient multiplications, coupled with a 24KB near-threshold SRAM. A State Assembler updates and coordinates Δ RNN states. At $\Delta_{TH} = 0.2$, the Δ RNN achieves 87% temporal activation sparsity, leading to a computing latency of 6.9ms@125kHz, 2.4 \times faster than the 16.4ms baseline at $\Delta_{TH} = 0$.

Figure 3 describes the serial IIR BPF-based FEx¹¹ circuit that includes a 4th-order IIR BPF implemented as a cascade of two second-order sections (**SOS**). Unlike most prior arts relying on 16b high-resolution ADCs, the IIR digital FEx interfaces with a 12b-quantized input audio signal, being compatible with low-power/low-area 12b ADCs. By reducing the IIR filter channels from 16 to 10, we retain KWS accuracy and cut FEx power consumption by 30%. The circuit is reconfigurable, supporting configurations from 1 to 16 channels. In addition, the filter coefficients are realized with 12b/8b mixed-precision, obtaining 2.4× power and 2.6× area reduction. Furthermore, the hardware-friendly properties (i.e., equivalence) of the a and b coefficients of the biquad filters are exploited so that half of the multipliers can be replaced with bit shifts, leading to 1.8× power and 1.8× area reduction. Putting all together, the power and area of the proposed digital FEx are reduced by 5.7× and 4.7×, respectively.

Figure 4 illustrates a 24KB weight SRAM operating at the 0.6V near-threshold voltage, which is divided into 12 banks of 2KB units each (Figure 1). The SRAM comprises 4 blocks (**BLKs**) of memory, a 10b address (**A**) register, a 16b input (**D**) register, a 0.6V-to-0.65V output (**Q**) level shifter for Δ RNN interfacing, and a skew-resistant column multiplexer (**MUX**). The proposed SRAM deploys the pitch-matched 6T level shifters that align with the 8T bitcell's vertical pitch to convert word lines (**WL/RWL**) from 0.6V to 1.2V leading to enhanced access time and static noise margin. Unlike prior art by Verma et al. relying on additional off-chip above-VDD WL booster¹², the proposed SRAM features an on-chip-integrated voltage booster (**VDDH**)¹³. Our combination approach of pitch-matched level shifter and voltage booster is distinct from Verma et al.¹³, which utilized the booster only for the read-buffer footer rather than word lines. The SRAM operates at reduced leakage power by employing high-VTH devices for bit cells. The column MUX uses dynamic NOR logic¹⁴ and a clock-skew-robust pre-charging scheme (**PCHCMX**), ensuring data (Q) refreshes at the falling clock edge and facilitating easier integration of full-custom design with synthesized logic. The SRAM achieves a 6.6× lower read power of 0.93 μ W (only 18% of the total power) and a 2× larger area than the push-rule foundry SRAM.

MEASUREMENT RESULTS

The FEx produces 12b 10-channel features from Mel-scale IIR BPFs, ranging from 516Hz to 4.22kHz. The Δ RNN, with its temporal sparsity, adjusts for accuracy, energy, and latency. It reduces latency by 2.4× to 6.9ms and energy by 3.4× to 36.11nJ/Decision, across $\Delta_{TH} = 0$ to 0.2 while maintaining >90% accuracy on the 11-class GSCD. As shown in Figure 5, the measured SRAM waveform indicates that the skew-resistant pre-charging scheme ensures Q data is always updated near the falling clock-edge. Our digital FEx features 12-bit input precision, seamlessly interfacing with low-power/low-area 12-bit ADCs, setting it apart from prior works relying on 16-bit high-resolution ADCs. The 65nm CMOS KWS IC integrates an IIR BPF-based FEx, Δ RNN accelerator, and 24KB near-threshold SRAM, occupying 0.084mm², 0.319mm², and 0.381mm² respectively (0.78mm² in total).

The IIR BPF-based FEx, Δ RNN accelerator, and near-threshold SRAM consume 25%, 57%, and 18% of the total power, respectively (Figure 6). Our processor achieves the best figure of merit (**FoM**) compared with^{2,5,15,16}, taking into account the number of keywords, energy per decision, error rate, and chip area.

ACKNOWLEDGMENTS

This work was partially supported by the Swiss National Science Foundation CA-DNNEdge project (208227) and Bridge project VIPS (181010).

REFERENCES

- [1] Weiwei Shan, Minhao Yang, Jiaming Xu, Yicheng Lu, Shuai Zhang, Tao Wang, Jun Yang, Longxing Shi, and Mingoo Seok. 14.1 a 510nw 0.41v low-memory low-computation keyword-spotting chip using serial fft-based mfcc and binarized depthwise separable convolutional neural network in 28nm cmos. In *2020 IEEE International Solid-State Circuits Conference - (ISSCC)*, pages 230–232, 2020.
- [2] Kwantae Kim, Chang Gao, Rui Graça, Ilya Kiselev, Hoi-Jun Yoo, Tobi Delbruck, and Shih-Chii Liu. A 23 μ w solar-powered keyword-spotting asic with ring-oscillator-based time-domain feature extraction. In *2022 IEEE International Solid-State Circuits Conference (ISSCC)*, volume 65, pages 1–3, 2022.
- [3] Kwantae Kim, Chang Gao, Rui Graça, Ilya Kiselev, Hoi-Jun Yoo, Tobi Delbruck, and Shih-Chii Liu. A 23- μ w keyword spotting ic with ring-oscillator-based time-domain feature extraction. *IEEE Journal of Solid-State Circuits*, 57(11):3298–3311, 2022.
- [4] Hassan Dbouk, Sujan K. Gonugondla, Charbel Sakr, and Naresh R. Shanbhag. A 0.44- μ j/dec, 39.9- μ s/dec, recurrent attention in-memory processor for keyword spotting. *IEEE Journal of Solid-State Circuits*, 56(7):2234–2244, 2021.

- [5] Ji-Hwan Seol, Heejin Yang, Rohit Rothe, Zichen Fan, Qirui Zhang, Hun-Seok Kim, David Blaauw, and Dennis Sylvester. A $1.5\mu\text{W}$ end-to-end keyword spotting soc with content-adaptive frame sub-sampling and fast-settling analog frontend. In *2023 IEEE International Solid-State Circuits Conference (ISSCC)*, pages 1–3, 2023.
- [6] Daniel Neil, Jun Haeng Lee, Tobi Delbruck, and Shih-Chii Liu. Delta networks for optimized recurrent network computation. In Doina Precup and Yee Whye Teh, editors, *Proceedings of the 34th International Conference on Machine Learning*, volume 70 of *Proceedings of Machine Learning Research*, pages 2584–2593. PMLR, 06–11 Aug 2017.
- [7] Chang Gao, Daniel Neil, Enea Ceolini, Shih-Chii Liu, and Tobi Delbruck. DeltaRNN: A Power-efficient Recurrent Neural Network Accelerator. In *Proceedings of the 2018 ACM/SIGDA International Symposium on Field-Programmable Gate Arrays*, FPGA '18, page 21–30, New York, NY, USA, 2018. Association for Computing Machinery.
- [8] Chang Gao, Antonio Rios-Navarro, Xi Chen, Shih-Chii Liu, and Tobi Delbruck. EdgeDRNN: Recurrent Neural Network Accelerator for Edge Inference. *IEEE Journal on Emerging and Selected Topics in Circuits and Systems*, 10(4):419–432, 2020.
- [9] Shih-Chii Liu, Chang Gao, Kwantae Kim, and Tobi Delbruck. Energy-efficient activity-driven computing architectures for edge intelligence. In *2022 International Electron Devices Meeting (IEDM)*, pages 21.2.1–21.2.4, 2022.
- [10] Fabrizio Ottati, Chang Gao, Qinyu Chen, Giovanni Brignone, Mario R. Casu, Jason K. Eshraghian, and Luciano Lavagno. To spike or not to spike: A digital hardware perspective on deep learning acceleration. *IEEE Journal on Emerging and Selected Topics in Circuits and Systems*, 13(4):1015–1025, 2023.
- [11] Qinyu Chen, Yaoxing Chang, Kwantae Kim, Chang Gao, and Shih-Chii Liu. An area-efficient ultra-low-power time-domain feature extractor for edge keyword spotting. In *2023 IEEE International Symposium on Circuits and Systems (ISCAS)*, pages 1–5, 2023.
- [12] Ik Joon Chang, Jae-Joon Kim, Sang Phill Park, and Kaushik Roy. A 32kb 10t subthreshold sram array with bit-interleaving and differential read scheme in 90nm cmos. In *2008 IEEE International Solid-State Circuits Conference - Digest of Technical Papers*, pages 388–622, 2008.
- [13] Naveen Verma and Anantha P. Chandrakasan. A 65nm 8t sub-vt sram employing sense-amplifier redundancy. In *2007 IEEE International Solid-State Circuits Conference. Digest of Technical Papers*, pages 328–606, 2007.
- [14] Shourya Gupta, Kirti Gupta, Benton H. Calhoun, and Neeta Pandey. Low-power near-threshold 10t sram bit cells with enhanced data-independent read port leakage for array augmentation in 32-nm cmos. *IEEE Transactions on Circuits and Systems I: Regular Papers*, 66(3):978–988, 2019.
- [15] Charlotte Frenkel and Giacomo Indiveri. Reckon: A 28nm sub-mm² task-agnostic spiking recurrent neural network processor enabling on-chip learning over second-long timescales. In *2022 IEEE International Solid-State Circuits Conference (ISSCC)*, volume 65, pages 1–3, 2022.
- [16] Atsutake Kosuge, Rei Sumikawa, Yao-Chung Hsu, Kota Shiba, Mototsugu Hamada, and Tadahiro Kuroda. A 183.4nj/inference 152.8 μW single-chip fully synthesizable wired-logic dnn processor for always-on 35 voice commands recognition application. In *2023 IEEE Symposium on VLSI Technology and Circuits (VLSI Technology and Circuits)*, pages 1–2, 2023.

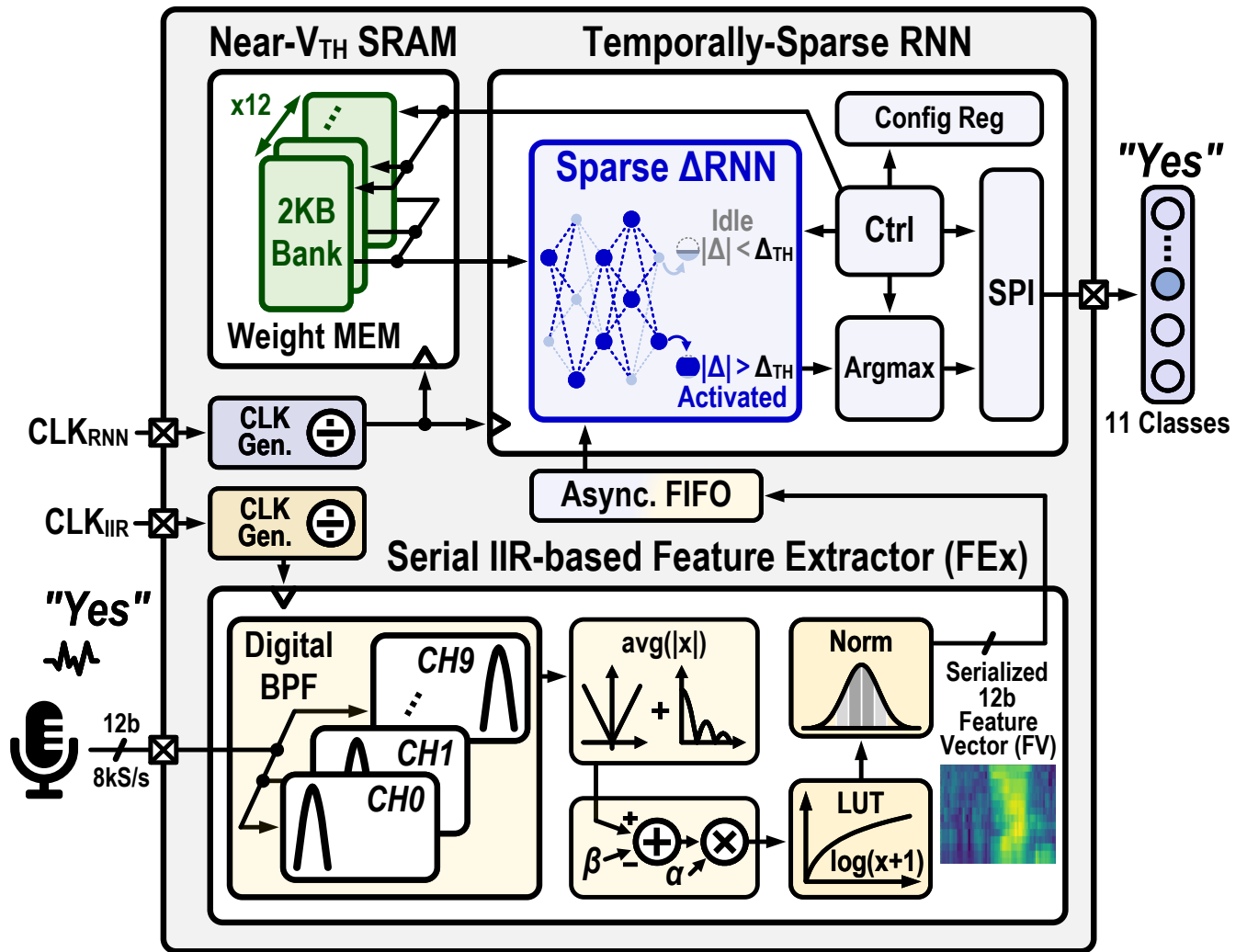


Figure 1: Overall architecture of proposed temporally-sparse Δ RNN KWS IC with IIR BPF-based time-domain FEx and near-threshold weight SRAM.

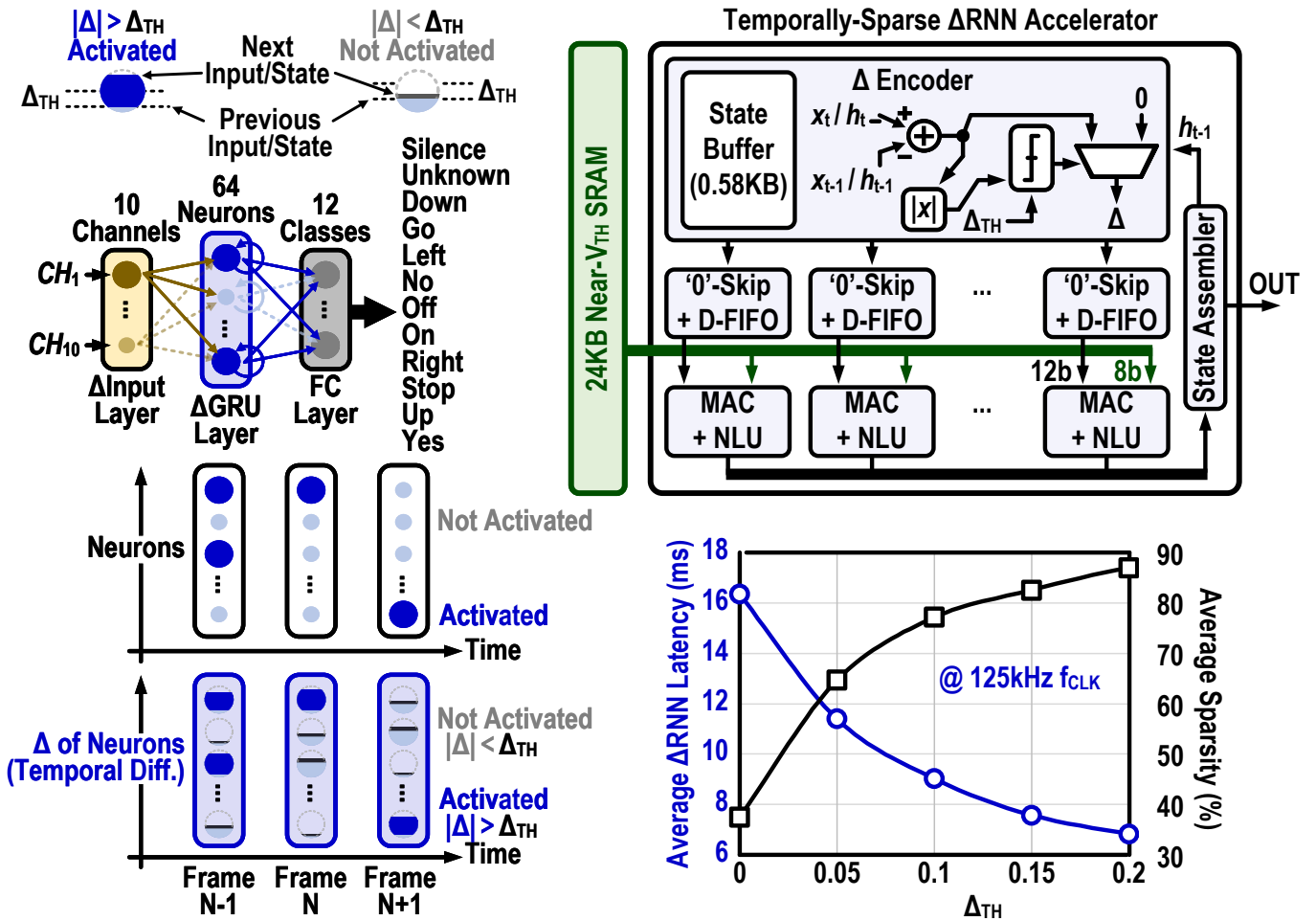


Figure 2: Concept of Δ RNN (left column), the architecture of the Δ RNN accelerator, average Δ RNN inference latency, and temporal sparsity for Δ_{TH} at 125kHz (right column).

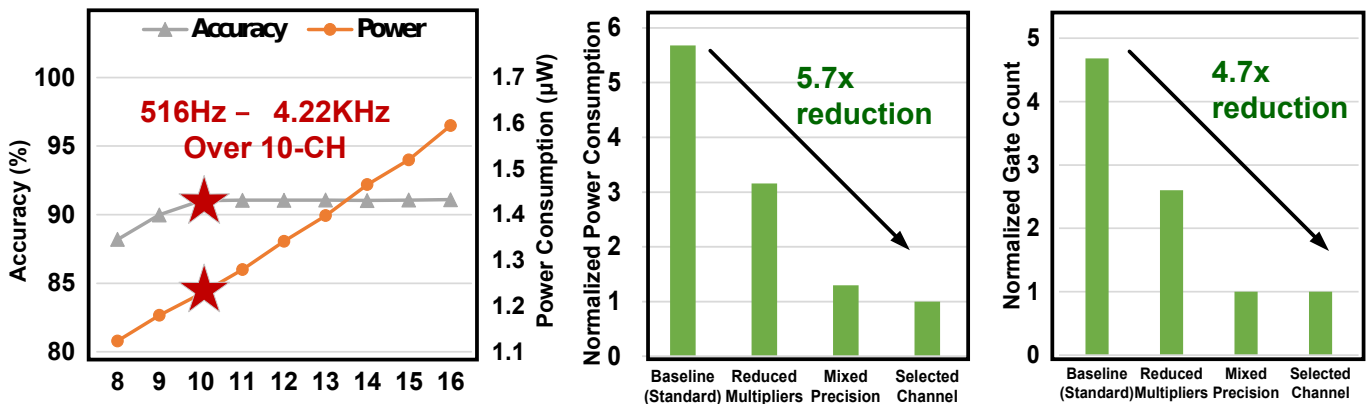
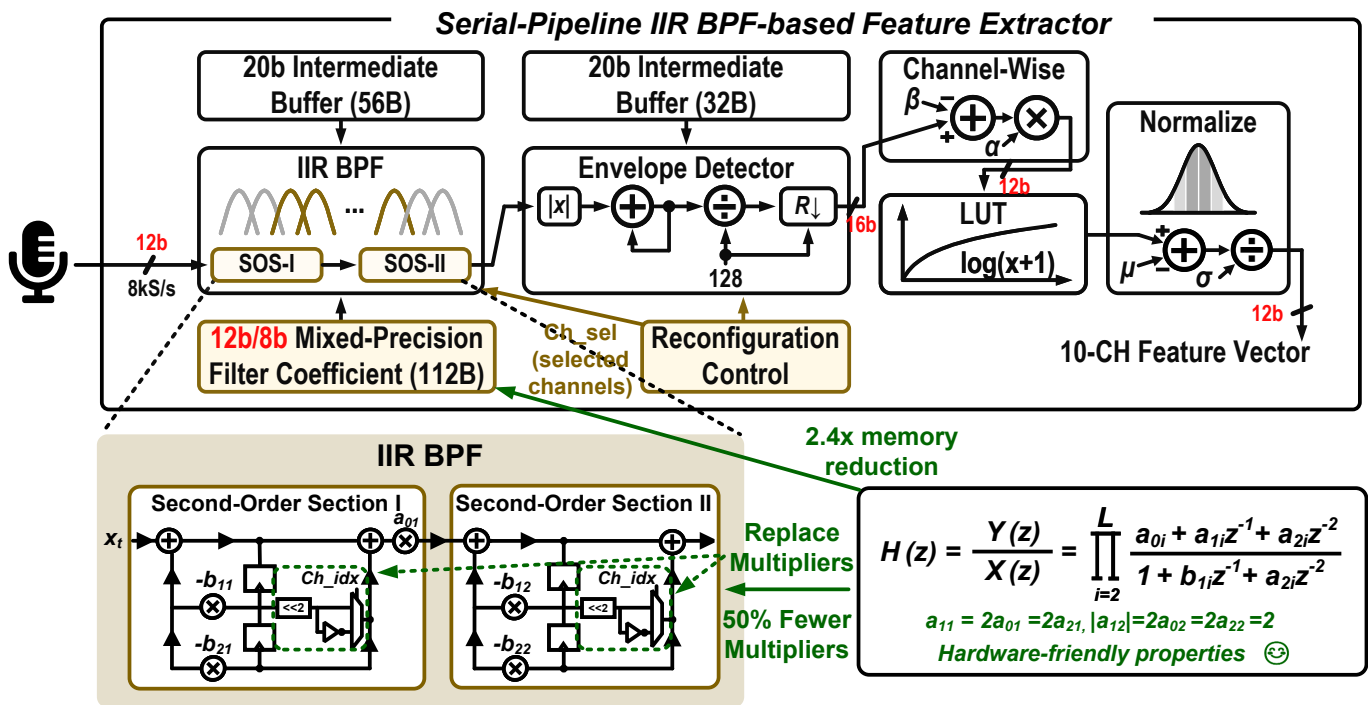


Figure 3: Concept and architecture of the serial time-domain IIR BPF-based FE. Simulated power vs. KWS accuracy over different # of channels, power consumption optimization, and area (gate count) optimization over each optimization step.

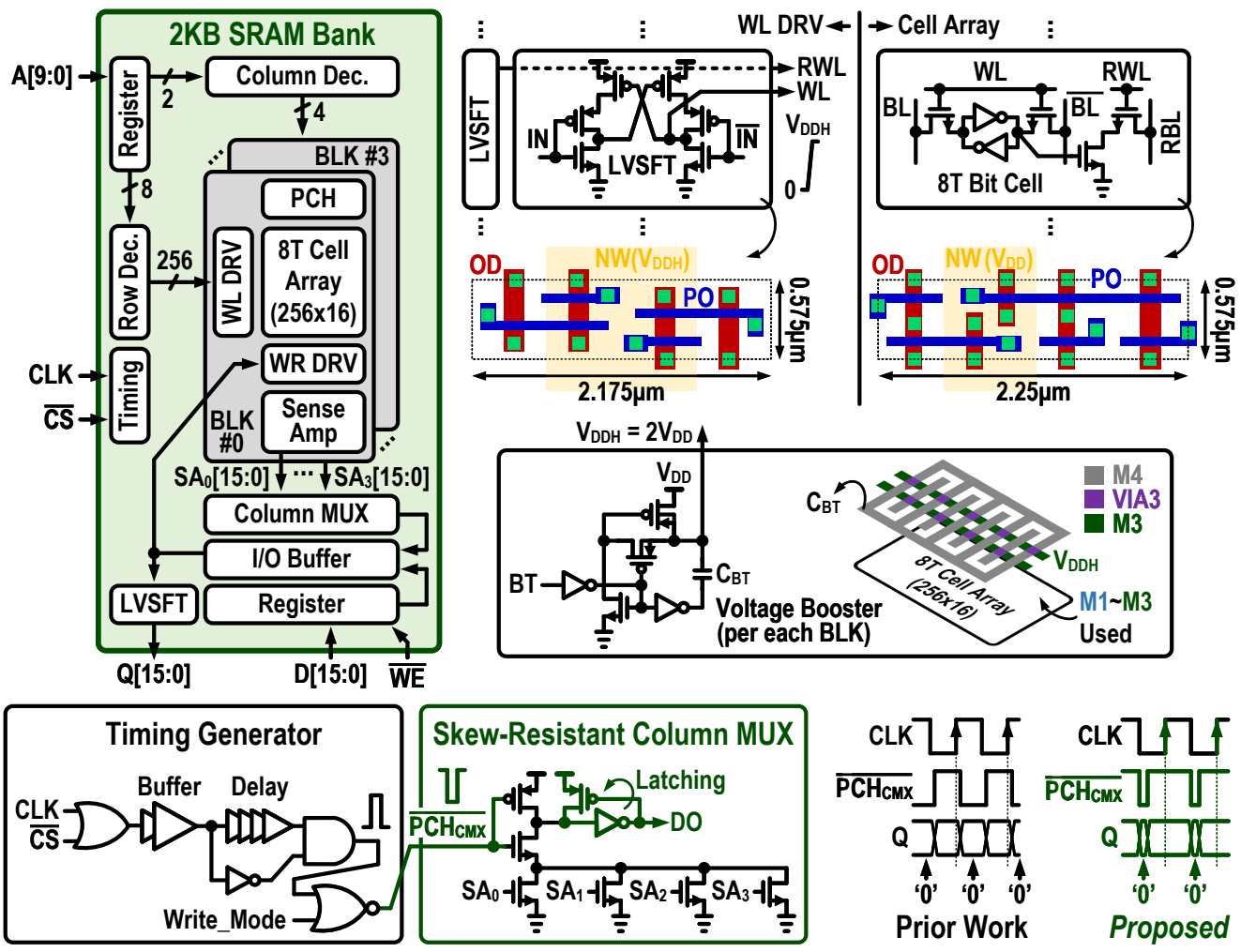


Figure 4: 0.6V near-threshold full-custom SRAM with pitch-matched level shifter, integrated voltage booster, timing generator, and skew-resistant column MUX.

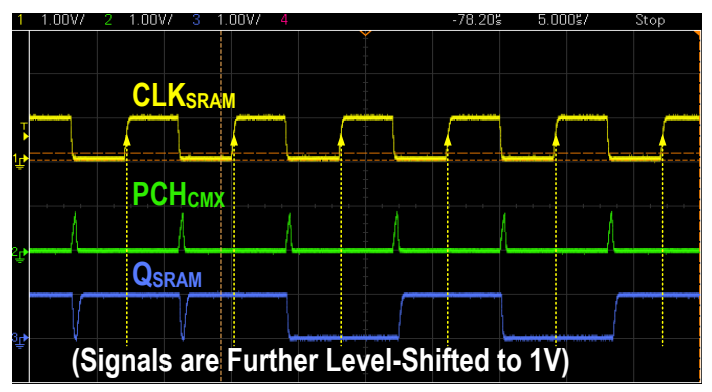
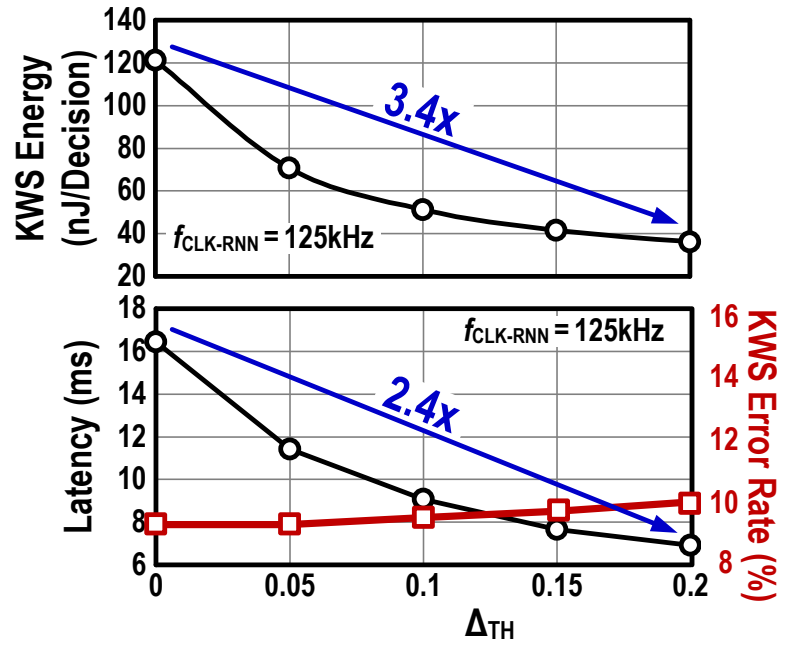
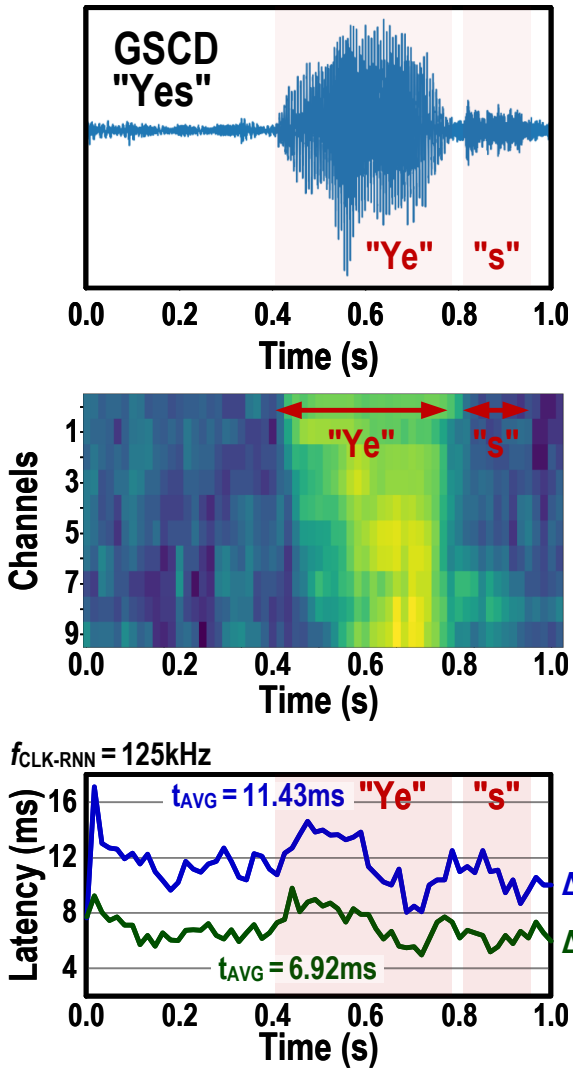
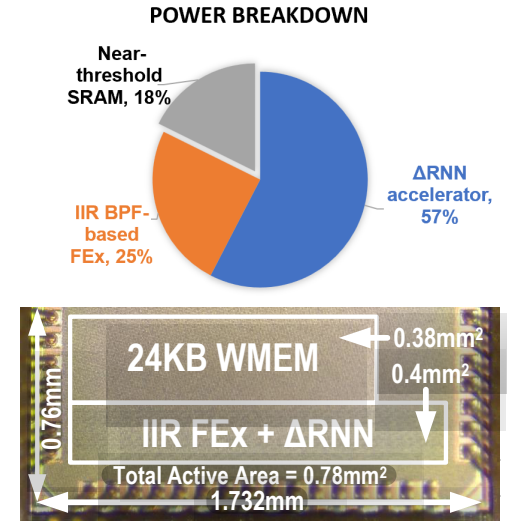


Figure 5: Measurement results. The audio waveform of GSCD "Yes," IIR features, Δ_{RNN} latency for two Δ_{TH} (left column). Energy/decision and total system power (upper right). Average computing latency with KWS error rates versus Δ_{TH} (middle right). Skew-resistant column MUX measurement from SRAM (lower right).

Digital FEx.	Shan ISSCC'20	Giraldo JSSC'20	This Work
Process(nm)	28	65	65
Area(mm ²)	0.057	0.66	0.084
Clock(Hz)	40k	250k	128k
Input Precision	16 bits	10 bits ^A	12 bits
Feature Precision	8 bits	8 bits	12 bits
Feature Type	MFCC	MFCC	IIR
Feature Dim.	8	<=32	<=16
Backbone	256-point FFT	512-point FFT	IIR-BPF
Freq. Range(Hz)	16-8k	<8k	100-7.9k
Supply(V)	0.41	0.6/0.8	0.65
Power(μ W)	0.34	7.2 ^B	1.22 ^C
Frame Shift(ms)	16	16	16
Serial FEx.	Yes	No	Yes

^A On-chip ADC ^B Measured with 13-D features ^C Measured with 10-D features



KWS	Kim ISSCC'22	Frenkel ISSCC'22	Seol ISSCC'23	Kosuge VLSI'23	This Work	
Process(nm)	65	28	28	40	65	
Supply(V)	0.5/0.75	0.5	1.4/0.65/0.5	0.5	0.6/0.65	
Area(mm ²)	2.03	0.45	0.8	7.63	0.78	
On-Chip Memory(KB)	27	138	18	0	26.3	
Clock(Hz)	250k	13M	1M	120k	125k	
Feature Ex.	Analog Time	No FEx	Digital Freq.	No FEx	Digital Time	
Algorithm	RNN	Spiking RNN	Skip RNN	CNN	Δ GRU-FC	
					$\Delta_{TH=0}$	$\Delta_{TH=0.2}$
Energy/Decision (nJ)	285.20	42	23.68	183.4	121.2	36.11
Comp. Latency(ms)	12.4	5.7	16	1.2	16.4	6.9
KWS Power(μ W)	23	79	1.48 ^A	152.8	7.36	5.22
Dataset	GSCD	SHD ^B	GSCD	GSCD	GSCD	
# Classes(Keywords)	12 (10)	2 (1)	7 (5)	35 (35) 10 (10)	11 (10)	
Accuracy(%)	86.03	90.7	92.8	78.2 88.0	91.1	90.5
FoM ^C	0.123	0.569	3.66	0.115 0.06	1.19	3.74

^A Power includes AFE, FE, and NN ^B Spiking Heidelberg Digits ^C FoM = $\frac{\# \text{ of keywords}}{\text{Error Rate}(\%) * \text{Energy/Decision (nJ)} * \text{Area}(\text{mm}^2)}$

Figure 6: Comparison tables, power breakdown, and die photo. Digital FEx (upper) and KWS ICs (lower).